ORIGINAL ARTICLE Neuroradiology

Whole tumor MR Perfusion histogram analysis in the preoperative assessment of patients with gliomas: Differentiation between high- and low-grade tumors

Vasileios K. Katsaros[1,2], Katerina Nikiforaki[3], Giorgos Manikis[4],
Kostas Marias[4], Evangelia Liouta[2], Christos Boskos[2], George Kyriakopoulos[5],
George Stranjalis[2], Nikolaos Papanikolaou [3]

[1]Department of MRI, General Anti-Cancer and Oncological Hospital of Athens "St. Savvas", Athens, Greece
[2]Department of Neurosurgery, Medical School, University of Athens,
General Hospital of Athens "Evangelismos", Athens, Greece
[3]Department of Copmutational Imaging, Champalimaud Foundation, Lisbon, Portugal
[4]Computational Medicine Laboratory, Institute of Computer Science, FORTH, Heraklion, Greece
[5]Department of Pathology, General Hospital of Athens "Evangelismos", Athens, Greece

Abstract

Purpose: To compare the diagnostic accuracy of normalized Blood Volume (nBV) histogram metrics in differentiating low from high-grade gliomas.

Material and Methods: Forty-four patients (22 female, 22 male) with histologically confirmed gliomas were included. Group A comprised 10 patients with low grade gliomas (all grade II) while group B comprised 34 patients (4 grade III and 30 grade IV). Three-dimensional whole tumor segmentation was based on intensity level clustering in T2 FLAIR for the non-enhancing lesions or post contrast T1 weighted images for the enhancing lesions. Dynamic Susceptibility Contrast (DSC) perfusion was applied in all patients, and leak-age corrected nBV maps were created. Corresponding histograms were generated from all the pixels included in the tumor volume. Minimum, maximum, mean, standard deviation, median, skewness, kurtosis, 5%, 30%, 70% and 95% percentiles, as well as normalized peak height and maximum peak position derived from normalized blood volume histograms were calculated for both groups. ROC analysis was performed to find optimum thresholds for differentiating between low and high grade gliomas.

Results: 5% percentile of nBV normalized histogram provided the highest area under the curve (AUROC: 0.93) for the differentiation of low from high grade gli-

CORRESPONDING AUTHOR, GUARANTOR

V. K. Katsaros, MD, Ph.D
Department of MRI, General Anti-Cancer and Oncological Hospital of Athens
"St. Savvas", Alexandras Avenue 119, Greece
E-mail: bslkatsaros@gmail.com

omas. A threshold value of 0.07 for the 5% percentile of nBV normalized histogram resulted in 90.8% sensitivity and 90% specificity. The positive and negative predictive values were 96.7% and 75%, respectively while the accuracy reached 91%. When removing 2 IDH mutation positive HGG patients, the corresponding AU-ROC increased to 0.98.

Conclusion: Whole tumor normalized Blood Volume histogram analysis proved to be a very accurate method to differentiate low from high grade gliomas.

KEY WORDS	brain tumors; perfusion; dynamic susceptibility weighted imaging; nBV

1. Introduction

Magnetic resonance (MR) imaging is the gold standard imaging modality for pre-operative assessment of patients with brain tumors. Although post gadolinium T1 weighted images are routinely used to evaluate the presence and pattern of enhancement, it has been shown that this method is not reliable in the assessment of tumor grading in certain cases [1, 2]. Alternative modalities like diffusion, perfusion imaging and MR spectroscopy were investigated whether they can improve accurate glioma grading classification with variable results [3-7].

Perfusion MR imaging involves the use of bolus injection of paramagnetic contrast agent during a dynamic sequence acquisition to derive relative cerebral blood volume (rCBV), relative cerebral blood flow (rCBF), time to peak (TTP) and mean transit time (MTT) maps. Several studies have shown that the maximal rCBV of gliomas correlates with the glioma grade [8–11]. Since absolute quantification of rCBV is not reproducible in the clinical setting, differentiation of high-grade gliomas (HGGs) and low-grade gliomas (LGGs) is based on measurement of the ratio between the most elevated rCBV area within the glioma, known also as the "hot-spot" method, and the rCBV of unaffected tissue, usually the contralateral normal appearing white matter. This value is often referred to as the normalized BV (nBV), and HGGs tend to have significantly higher nBVs than LGGs [11]. It should be noted, however, that this approach has some inherent limitations. The selection of a glioma hot spot is highly user dependent because differentiation between vessels and the tumor region of true blood volume elevation can be challenging and a source of potential error. Moreover, since only a few image pixels are typically used to determine the rCBV hot spot, the method is inherently sensitive to image noise and other sources of spurious pixel values (e.g., partial volume averaging with leptomeningeal vessels, spikes introduced by the algorithms used to generate the nBV maps). Additionally, unaffected white matter rCBV is generally used to derive the normalized CBV. This is based on the assumption that most gliomas are located in the white matter. However, incorrect selection of reference rCBVs (e.g. regions affected by vasculopathy) might result in either under- or overestimation of normalized CBVs. In the current study, a more comprehensive method to extract the quantitative information from the corresponding imaging biomarkers (nBV) was performed [12]. Contrary to the "hot-spot" method, the proposed histogram analysis is based on information derived from the whole tumor combined with sophisticated segmentation algorithms and has the potential to improve diagnostic efficacy. In order to avoid tumor size bias the histograms were transformed in normalized histograms keeping the area under the histogram equal to one.

The purpose of our study was to assess the diagnostic accuracy of whole tumor nBV normalized histogram metrics in differentiating low- from high-grade gliomas.

2.Material and Methods

2.1 Patient Demographics

The local ethics committee approved the present retrospective study. Patient consent was waived since our clinical glioma protocol included a DSC perfusion sequence and nBV maps, are part of the pre-surgical standard glioma evaluation. Our clinical glioma protocol also included Magnetization Prepared Rapid Acquisition Gradient Echo (MPRAGE) 3D-T1-weighted (TR 2,400 ms, TE 3.5 ms, TI 1000 ms, FOV 240 mm x 240 mm, flip angle 8^0, bandwidth 180 Hz/Px, isotropic voxel (size 1.2 mm³), 160-176 slices, TA 7:42 min) in sagittal plane, 2D-FLAIR-BLADE (for

motion correction) (TR 10,000 ms, TE 89 ms, FOV 240 mm x 240 mm, slice thickness 2 mm, 60 slices, TA 4:48 min), T2-weighted- BLADE (for motion correction) (TR 4,000 ms, TE 107 ms, FOV 240 mm x 240 mm, slice thickness 3 mm, 40 slices, TA 4:36 min) and gradient echo (GRE) T2* (TR 959 ms, TE 26 ms, FOV 240 mm x 240 mm, slice thickness 5 mm, 24 slices, TA 4:56 min) in axial plane, as well as MPRAGE 3D-T1-weighted post-gadolinium sequences.

Forty-four consecutive patients (22 males, 22 females; mean age, 62 years; age range, 17–75 years) who had pre-operative MR imaging examination, no relevant treatment history at the time of imaging (such as radio-, chemo-, or antiangiogenic therapy), and consecutive histopathological diagnoses were included and retrospectively reviewed in the study. The tumor grading was based on World Health Organization criteria and yielded 10 low-grade gliomas (all grade II - Group A) and 34 high-grade (4 grade III and 30 grade IV- Group B).

2.2 Conventional MR Imaging

Conventional MR imaging and DSC were performed during the same examination session to allow direct comparison and image registration. The imaging was performed on a 1.5T MR imaging scanner (Magnetom Symphony/ Vision; Siemens, Erlangen, Germany) equipped with a 4-channel receiver head coil. Before the examination, a 16- to 20-G needle was inserted in either the right or the left antecubital vein. Consequently, isotropic 3D-MPRAGE T1-weighted sagittal, FLAIR, GRE T2* and T2-weighted axial images were acquired (*see above*).

2.3 DSC MR Imaging

A gadolinium-based agent (Gadobutrol, Gadovist; Bayer, Germany) was intravenously injected at a dose of 0.1 ml per kilogram of body weight, followed by a 20-ml saline flush. Standard gradient echo echo-planar images were consecutively acquired (TR 1,370 ms, TE 35 ms, flip angle 60^0, section thickness 5 mm, FOV 240 mm x 240 mm, acquisition matrix 128x128 interpolated to 256x256).

2.4 Histopathology

Pathological examination was performed in the specimens obtained from surgical procedures, using classic hematoxylin-eosin stains plus immunohistochemical stains for the mutated form of isocitrate dehydrogenase (IDH1^{R132H}, Dianova), for the Glial fibrillary acidic protein (GFAP, DAKO), for the proliferation index ki-67 (DAKO) and for the onco-

protein *p*53 (DAKO). The presence of pleomorphism, atypia, mitosis, necrosis, astrogliosis, and macrophage infiltration were noted for each patient. For statistical purposes, all glial tumors were categorized as LGGs (grades I–II) and HGGs (grades III–IV) by using World Health Organization 2007 classification. Diffuse astrocytomas and DNET were classified as LGG. Anaplastic astrocytomas and glioblastomas multiforme (GBM) were classified HGG. Low- and high-grade oligodendrogliomas were evaluated as non-astrocytic tumors.

2.5 Post Processing

All imaging data where transferred through a secure website to our remote image processing labs. Image analysis was performed on DSC data by means of a dedicated software package (Tumor EX, Nordic NeuroLabs, Bergen, Norway). Initially, motion correction was applied on the DSC data to improve image quality and remove problematic dynamics with increased motion that might reduce the accuracy of the calculated nBV values. Following to that, a co-registration algorithm was applied to the DSC T2, T2 FLAIR and post contrast T1 weighted sequences. Then, a classification algorithm was used to segment the pixels, that were belonging to the tumor based on intermediate to high signal intensities on FLAIR and high signal intensities on post gadolinium T1 weighted images. The methodology followed in the current study is described in detail by Emblem et al. [12]. Normalized Blood Volume maps were reconstructed on a pixel-by-pixel basis using the whole brain tissue (excluding the tumor on a semi-automatic basis) and the corresponding whole tumor histograms were generated by including the nBV values from the tumoral pixels as identified from the segmentation algorithm. Finally nBV histogram normalization was done by normalizing the area under the histogram to a unity, and normalized peak height and maximum peak position were computed.

2.6 Statistical Analysis

Several normalized histogram metrics were calculated including: Minimum, maximum, mean, standard deviation, median, 5%, 30%, 70% and 95% percentiles, as well as, normalized peak height and maximum peak position for both groups. Mann-Whitney U test was applied to investigate for statistically significant differences between group A (LGG) and B (HGG) for each individual metric with a threshold of *p*<0.05.
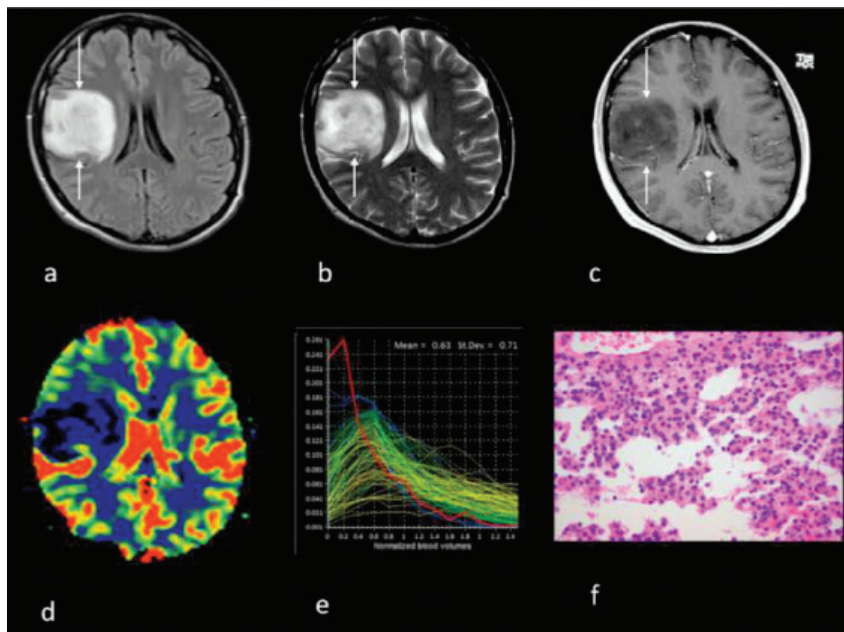
Fig. 1. *Patient with diffuse anaplastic astrocytoma Grade II of the right frontal lobe (arrows) shows heterogeneous increased signal intensity compared to the normal parenchyma of the brain in T2-W and FLAIR sequences (**a,b**), no enhancement of the lesion in T1w image after intravenous administration of gadolinium (**c**) and lower nBV in DSC perfusion imaging (**d**) compared to the contralateral hemisphere. The nBV histogram (**e**) analysis shows the typical curve (red line shifted to the left upper side of the y axis) for a low grade glioma. Histopathology shows diffuse fibrillary astrocytoma grade II (Haematoxyline Eosine (HE) stain) characterized by modest hypercellularity, nuclear pleomorphism, and numerous small microcysts (**f**)*
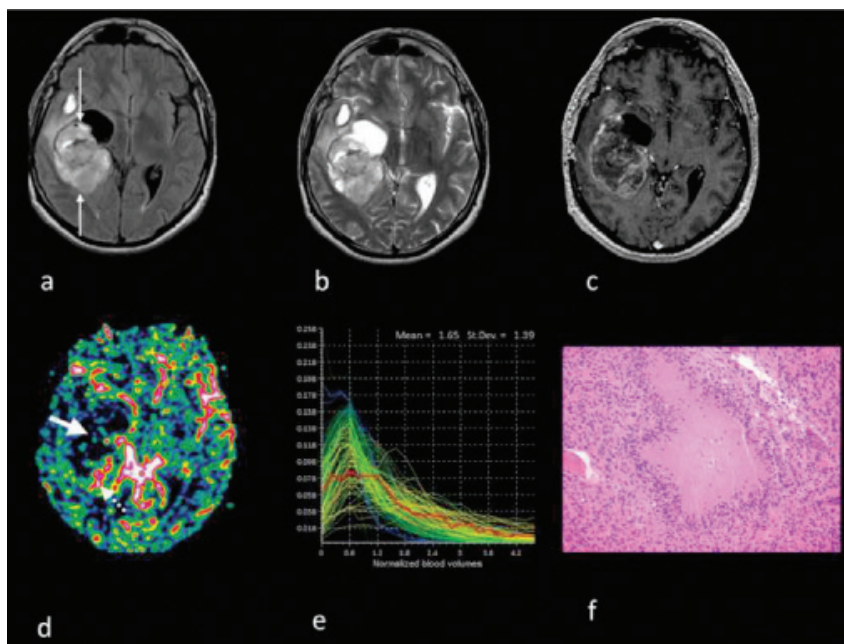

Fig. 2. *Patient with anaplastic oligodendroglioma (arrows). Heterogeneous appearance on FLAIR (**a**), T2 (**b**) and post gadolinium T1 weighted images (**c**). On the nBV map there are areas of high nBV values (dashed arrow) and areas of low nBV values (arrowhead) (**d**). The histogram (**e**) is containing more low nBV values (red line) but also a number of high nBV values up to 4.2. HE stain reveals anaplastic focus with a central subnecrotic area (**f**). The cells in this focus are smaller and denser than in the quiescent portion. The extensive capillary network, typical of oligodendrogliomas, is clearly visible in both parts of the tumor*
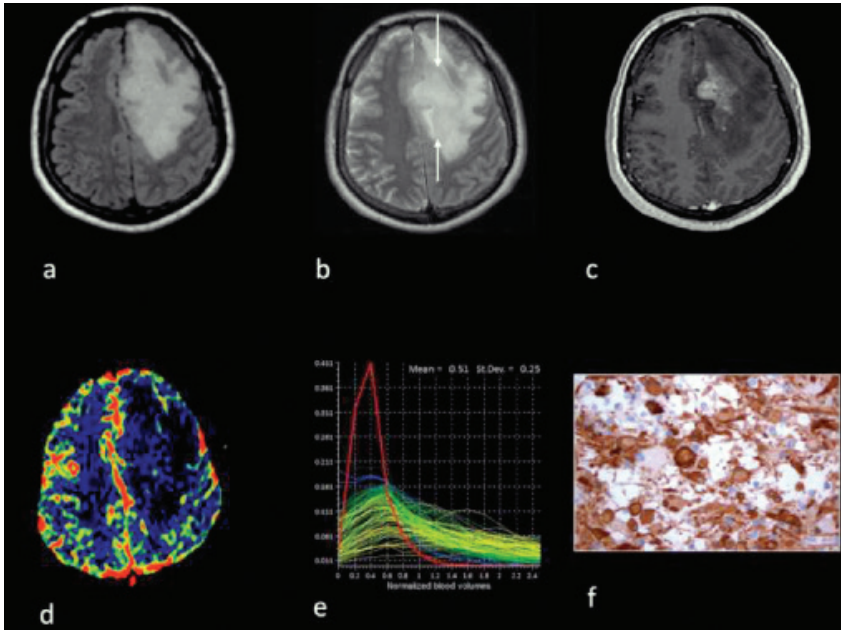
Fig. 3. *Patient with an anaplastic astrocytoma (based on immunohistochemistry) with universal expression of the mutated form of isocitric dehydrogenase (IDH) **(f)**. Extensive peritumoral edema is shown on axial FLAIR **(a)** and T2 TSE weighted images **(b)** while contrast enhancement is present on post gadolinium T1 TSE **(c)** images. nBV of the IDH mutation positive tumor **(d)** is lower than that of figure 2. The normalized nBV histogram (red line) also resembles that of a low-grade tumor **(e)** presenting the low nBV values in higher frequencies (peak shifted to the left side)*
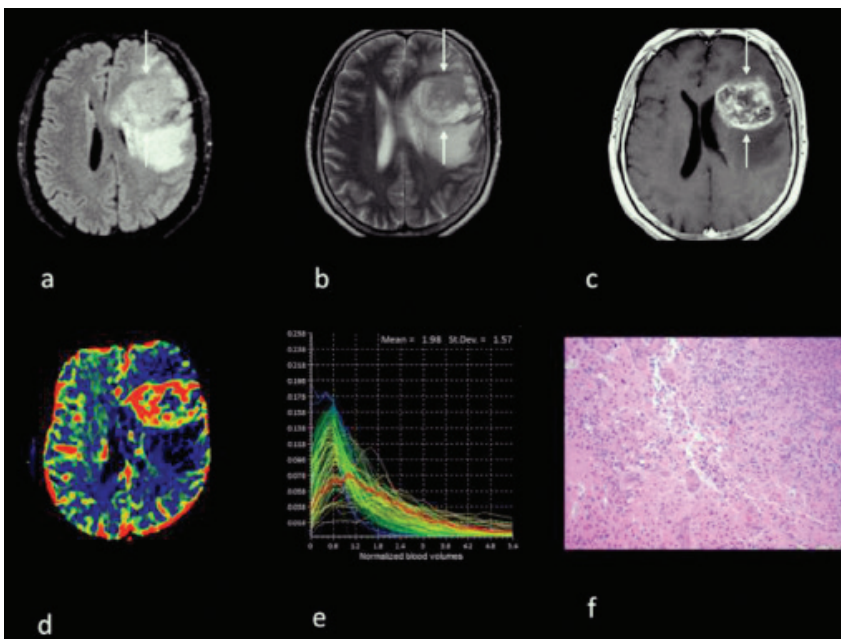

Fig. 4. *Patient with primary glioblastoma multiforme (arrows) with typical heterogeneous appearance on both FLAIR **(a)** and T2 weighted **(b)** images, and strong peripheral enhancement with central necrotic part as identified on post contrast T1 weighted image **(c)**. Significant vascular heterogeneity is shown on nBV map **(d)** that is reflected on the whole tumor normalized histogram (red line) **(e)** as a wide, low amplitude histogram containing various nBV values (low, moderate and high). **(f)** HE stain demonstrates multifocal sizeable "palisading" necrosis with "geographic" pattern. The proliferation marker ki-67 was elevated (40%)*

Table 1. Results of the statistical analysis including all histogram metrics that were evaluated

	Min		Max		Mean		Median		Skewness		Kurtosis	
	LGG	HGG	LGG	HGG	LGG	HGG	LGG	HGG	LGG	HGG	LGG	HGG
MIN	0.001	0.001	0.464	0.482	0.074	0.1374	0.061	0.132	0.49	0.10	2.19	-0.04
MAX	0.004	0.344	6.061	23.237	0.461	4.676	0.409	4.064	3.43	3.29	22.43	22.42
MEAN	0.0021	0.055	2.435	4.813	0.3196	1.203	0.26	1.073	2.08	1.22	11.95	4.75
p-value	0.001701454		1.017059191		0.000029111		0.000016514		0.024825989		0.015707352	
AUROC	0.738		0.70		0.867		0.882		0.751		0.785	
Threshold	0.0055		3.286		0.4819		0.415		2.06		9.66	
Sensitivity	60.61%		60.60%		78.79%		78,79%		96,97%		96.97%	
NPV	43.48%		38.10%		58.82%		58.82%		85.71%		85.71%	
PPV	100%		90.91%		100%		100%		88.89%		88.89%	
Accuracy	69.77%		65.12%		83.72%		83.72%		88.37%		88.37%	

The aforementioned metrics were also analyzed to calculate the area under the curve of the receiver operating characteristics curves (AUROC). Sensitivity, specificity, negative and positive predictive values and accuracy were calculated and the optimal thresholds were recorded, using SPSS software and a $p<0.05$ as a threshold.

3. Results

In Group A the histopathological diagnosis was concordant with a complex Dysembryoplastic Neuro-Epithelial Tumor (DNET -WHO-Grade II) in 1 case, diffuse fibrillary astrocytoma (**Fig. 1**) in 6 cases, oligodendroglioma in 2 cases and mixed pattern of astrocytoma/oligodendroglioma in 1 case.

Group B comprised of 4 Grade III cases, 2 anaplastic oligodendrogliomas (**Fig. 2**) and 2 anaplastic astrocytomas, 1 of them demonstrating the IDH mutation (**Fig. 3**), as well as of 30 Grade IV cases, 4 Glioblastoma Multiforme (GBM) with oligodendroglial component and 26 GBM (25 primary (**Fig. 4**) and 1 secondary, the latter demonstrating also the IDH mutation).

Tables 1 and **2** are disclosing the descriptive statistics of all metrics derived from nBV normalized histograms, as well as, the diagnostic performance of each individual metric for the differentiation between low and high-grade gliomas. All normalized histogram metrics provided statistically significant differences between low- and high-grade glioma groups ($p<0.05$, using the Mann-Whitney U test).

The most accurate normalized histogram metric to differentiate low- from high -grade gliomas was the 5% percentile nBV. In group A the 5% percentile nBV ranged between 0.001 and 0.117 (mean, 0.044 ± 0.03), while in group B ranged between 0.013 and 1.292 (mean, 0.344 ± 0.3), resulting in AUROC of 0.933 while a threshold value of 0.07 provided 90.91% sensitivity and 90% specificity. The positive and negative predictive values were 96.77% and 75%, respectively, while the accuracy reached 90.7%. The second most accurate normalized histogram metric was nBV peak position providing an AUROC of 0.918 while a threshold value of 0.06 provided 93.94% sensitivity and 80% specificity. The positive and negative predictive values were 93.94% and 80%, respectively while the accuracy reached 90.7%. A pairwise comparison between ROC curves of nBV 5% percentile and nBV peak position led to non-significant differences in AUROC (p=0.2253). When removing the 2 IDH mutation positive patients with high grade gliomas, the corresponding AUROC increased to 0.98, and keeping the same threshold of the 5% percentile, the sensitivity, specificity, PPV, NPV and accuracy became 100%, 90%, 96.77%, 100% and 97.5%, respectively (**Tables 1-2**).

4. Discussion

Accurate grading of gliomas is of paramount importance because the therapeutic approach and prognosis differ considerably according to tumor grade [1, 2, 13, 14]. Whereas conventional MR imaging provides information on contrast enhancement, mass effect, edema, and necrosis, it is not always accurate for the precise grading of gliomas [13].

Table 2. Results of the statistical analysis including all histogram metrics that were evaluated

	5%		30%		70%		95%		Peak Position		Peak Height	
	LGG	HGG	LGG	HGG	LGG	HGG	LGG	HGG	LGG	HGG	LGG	HGG
MIN	0.001	0.013	0.037	0.097	0.085	0.162	0.193	0.252	0.001	0.109	0.04	0.03
MAX	0.117	1.292	0.351	2.909	0.593	5.45	1.485	10.532	0.351	5.121	0.17	0.08
MEAN	0.044	0.34	0.173	0.776	0.380	1.436	0.793	2.514	0.158	0.95	0.08	0.04
p-value	0.000007660		0.000009609		0.000029869		0.000162892		0.000129827		0.014431878	
AUROC	0.933		0.886		0.861		0.812		0.918		0.888	
Threshold	0.0705		0.38		0.612		1.55		0.291		0.06	
Sensitivity	90.91%		72.73%		75.76%		63.64%		81.82%		93.94%	
Specificity	90%		100%		100%		100%		90%		80%	
NPV	75%		52.63%		55.56%		45.45%		60%		80%	
PPV	96.77%		100%		100%		100%		96.43%		93.94%	
Accuracy	90.70%		79.07%		81.40%		72.09%		83.72%		90.70%	

Previous studies have suggested that contrast enhancement alone is not sufficient to predict tumor grade [10] because some low-grade gliomas demonstrate contrast enhancement whereas some high-grade tumors do not [13, 14]. However, the extent of contrast enhancement has been traditionally used as a mark of malignancy [15, 16].

Advanced MR imaging techniques such as dynamic susceptibility contrast has been utilized for the assessment of brain tumors neovascularity [3-11, 14]. MR imaging perfusion methods allow the generation of CBV maps that are potentially useful in the characterization of gliomas because tumor aggressiveness and growth are associated with endothelial neovascularization. rCBV measurements have been correlated with tumor grade and histologic findings of increased tumor angiogenesis [14, 16, 17].

Previous published studies [9, 14, 17, 18] reported a range of normalized rCBV values from 1.11 to 1.69 and from 3.64 to 7.32 in low-grade and high-grade gliomas, respectively. Our nBV values (0.67 and 1.70, for low grade and high grade gliomas respectively,) were significantly lower due to the fact that normalization in the current study was based on both normal gray and white matter [12], while in the literature most researchers are using only white matter. Our denominator is higher due to the higher rCBV values of normal gray matter when comparing to rCBV values of white matter. Therefore the ratio in our study was systematically lower to what is usually presented in the literature [11-22].

Several studies [13, 20-22] have found statistically significant differences between high-grade and low-grade gliomas mean rCBV values using the "hot-spot" method, as was done by subjective evaluation on an individualized basis from an experienced in brain tumors neuroradiologist (VKK) also in the patients reported in this study. A large series published in 2004 by Law et al. [22] found an rCBV threshold value of 1.75 with a sensitivity of 95% and specificity of 57.5%. Another study published by Lev et al. [11] showed that as the threshold level is lowered, the specificity is decreased and some low-grade gliomas are falsely identified as high-grade and will be treated more aggressively [18]. In our study the two (2) low-grade oligodendrogliomas, as well as the one (1) oligoastrocytoma showed no increase of the nBV, as reported in the literature [19], nor a histogram compatible with high-grade glioma, while the two (2) anaplastic oligodendrogliomas demonstrated typical features of high grade glioma (**Fig. 2**).

On the basis of differences between high- and low-grade gliomas in terms of vascular heterogeneity, Emblem et al proposed an alternative method to differentiate HGG from LGG using nBV histogram analysis of the entire tumor volume [23]. Whole lesion histogram analysis represents a more comprehensive method of quantification and information extraction comparing to traditional two dimensional region of interest generation on a single slice. Apparently, histogram analysis does not suffer from personal bias, introduced by the person drawing the region of inter-

est, however it requires the availability of a robust and accurate segmentation algorithm. In addition, the final outcome of a 2D ROI based measurement method is a single number that is suffering from averaging effects especially when heterogeneous lesions are studied.

In comparison to previous reported data of nBV by histogram analysis limited by absence of image co-registration [23], we have found that the proposed histogram amplitude (peak height) evaluation derived lower AUROC, as well as sensitivity in our study in comparison to 5% percentile value. This difference of our data with recent reports [11, 13-22] could be attributed mostly to the different methodological approach and analysis of dynamic susceptibility weighted perfusion imaging we performed (3D nBV histogram quantification instead of two dimensional hot spot method of rCBV). In the current study, glioma grading was based on the differences of vascular heterogeneity that can be quantified by histogram metrics of whole tumor nBV [21, 22]. The histogram-based analysis has been further improved with parametric analysis not only of the histogram shape (minimum, maximum, mean, standard deviation, median, 5%, 30%, 70% and 95% percentiles) but also with analysis of different set of values (normalized peak height and maximum peak position).

In gliomas, IDH mutations appear to define a distinct clinical subset of tumors, as these patients have a significantly longer median survival compared to patients with wild-type IDH1 gliomas [24]. Glioma patients with mutations in the gene IDH1(showing in MR spectroscopy a peak of 2-HG) have a greater 5-year survival rate than patients with wild-type IDH gliomas (93% *vs.* 51%), suggesting that IDH mutations represent a clinically distinct subset of patients [24, 25]. Retrospectively, when we removed the two patients who showed IDH mutation in histopathology the diagnostic accuracy significantly improved reaching 97.5%. We could hypothesize that the improved results can be attributed to decreased regions of neovascularity in IDH-mutation positive gliomas in comparison to patients with wild-type IDH gliomas (histogram shift up and left in the y axis representing LGG and nbV Mean Value=0.51/ StDev 0.25) (**Fig. 3**). Taking into account this shortcoming, we should be cautious in the interpretation of the nBV histograms in this subtype of high-grade gliomas. Also further studies on nBV histogram analysis with more glioma patients carrying the IDH mutation are needed to correlate the production of the metabolite 2-HydroxyGlutarate (2-HG, possibly detected by MR Spectroscopy) [25] with any decreased proliferation of neo-vessels in these cases.

The most important limitation of our study was that the analysis was based on the differentiation of high- from low-grade gliomas. We did not assess changes between the different grades due to the small number of grade III tumors. The latter was also responsible for the adequate statistical power that was achieved to discriminate low- from high-grade tumors.

In conclusion, whole tumor nBV normalized histogram analysis seems to be an accurate method for the differentiation between low- and high-grade gliomas. **R**

Conflict of interest:
The authors declare that they have no conflict of interest.

REFERENCES

1. Lev MH, Rosen BR. Clinical applications of intracranial perfusion MR imaging. *Neuroimaging Clin N Am* 1999; 9(2): 309-331.
2. Law M, Oh S, Babb JS, et al. Low-grade gliomas: Dynamic susceptibility-weighted contrast-enhanced perfusion MR imaging prediction of patient clinical response. *Radiology* 2006; 238(2): 658-667.
3. Covarrubias DJ, Rosen BR, Lev MH. Dynamic magnetic resonance perfusion imaging of brain tumors. *Oncologist* 2004; 9(5): 528-537.
4. Yang D, Korogi Y, Sugahara T, et al. Cerebral gliomas: Prospective comparison of multivoxel 2D chemical-shift imaging proton MR spectroscopy,echoplanar perfusion and diffusion-weighted MRI. *Neuroradiology* 2002; 44: 656-666.
5. Al-Okaili RN, Krejza J, Woo JH, et al. Intra-axial brain masses: MR imaging-based diagnostic strategy-initial experience. *Radiology* 2007; 243(2): 539-550.
6. Ebisu T, Tanaka C, Umeda M, et al. Discrimination of brain abscess from necrotic or cystic tumors by diffusion-weighted echo planar imaging. *Magn Reson Imaging* 1996; 14: 1113-1116.

7. Stadnik TW, Chaskis C, Michotte A, et al. Diffusion-weighted MR imaging of intracerebral masses: Comparison with conventional MR imaging and histologic findings. *AJNR Am J Neuroradiol* 2001; 22: 969-976.

8. Edelman RR, Mattle HP, Atkinson DJ, et al. Cerebral blood flow: Assessment with dynamic contrast-enhanced T2*-weighted MR imaging at 1.5 T. *Radiology* 1990; 176(1): 211-220.

9. Aronen HJ, Gazit IE, Louis DN, et al. Cerebral blood volume maps of gliomas: Comparison with tumor grade and histologic findings. *Radiology* 1994; 191(1): 41-51.

10. Knopp EA, Cha S, Johnson G, et al. Glial neoplasms: Dynamic contrast-enhanced T2*- weighted MR imaging. *Radiology* 1999; 211(3): 791-798.

11. Lev MH, Ozsunar Y, Henson JW, et al. Glial tumor grading and outcome prediction using dynamic spin-echo MR susceptibility mapping compared with conventional contrast enhanced MR: Confounding effect of elevated rCBV of oligodendrogliomas. *AJNR Am J Neuroradiol* 2004; 25(2): 214-222.

12. Emblem KE, Nedregaard B, Nome T, et al. Glioma Grading by Using Histogram Analysis of Blood Volume Heterogeneity from MR-derived Cerebral Blood Volume Maps. *Radiology* 2008; 247: 808-817.

13. Rollin N, Guyotat J, Streichenberger N, et al. Clinical relevance of diffusion and perfusion magnetic resonance in assessing intra-axial brain tumors. *Neuroradiology* 2006; 48: 150-159.

14. Lee EJ, Lee SK, Agid R, et al. Preoperative grading of presumptive low-grade astrocytomas on MR imaging: Diagnostic value of minimum apparent diffusion coefficient. *AJNR Am J Neuroradiol* 2008; 29: 1872-1877.

15. McKnight TR, Lamborn KR, Love TD, et al. Correlation of magnetic resonance spectroscopic and growth characteristics within grade II and III gliomas. *J Neurosurg* 2007; 106: 660-666.

16. Law M, Yang S, Wang H, et al. Glioma grading: Sensitivity, specificity, and predictive values of perfusion MR imaging and proton MR spectroscopic imaging compared with conventional MR imaging. *AJNR Am J Neuroradiol* 2003; 24: 1989-1998.

17. Kim HS, Kim SY. A prospective study on the added value of pulsed arterial spin labeling and apparent diffusion coefficients in the grading of gliomas. *AJNR Am J Neuroradiol* 2007; 28: 1693-1699.

18. Hakyemez B, Erdogan C, Ercan I, et al. High-grade and low-grade gliomas: Differentiation by using perfusion MR imaging. *Clin Radiol* 2005; 60: 493-502.

19. Barajas RF Jr, Cha S. Benefits of dynamic susceptibility-weighted contrast-enhanced perfusion MRI for glioma diagnosis and therapy. *CNS Oncol* 2014; 3(6): 407-419.

20. Zonari P, Baraldi P, Crisi G. Multimodal MRI in the characterization of glial neoplasms: The combined role of single-voxel MR spectroscopy, diffusion imaging and echo-planar perfusion imaging. *Neuroradiology* 2007; 49: 795-803.

21. Law M, Yang S, Babb JS, et al. Comparison of cerebral blood volume and vascular permeability from dynamic susceptibility contrast-enhanced perfusion MR imaging with glioma grade. *AJNR Am J Neuroradiol* 2004; 25: 746-755.

22. Boxerman JL, Schmainda KM, Weisskoff RM. Relative cerebral blood volume maps corrected for contrast agent extravasation significantly correlate with glioma tumor grade, whereas uncorrected maps do not. *AJNR Am J Neuroradiol* 2006; 27: 859-867.

23. Emblem KE, Scheie D, Due-Tonnessen P.Histogram Analysis of MR Imaging–Derived Cerebral Blood Volume Maps: Combined Glioma Grading and Identification of Low-Grade Oligodendroglial Subtypes. *AJNR* 2008; 29: 1664-1670.

24. Yan H, Parsons DW, Jin G, et al. IDH1 and IDH2 mutations in gliomas. *N Engl J Med.* 2009; 360: 765-773.

25. Dang L, White DW, Gross S, et al. Cancer-associated IDH1 mutations produce 2-hydroxyglutarate. *Nature* 2009; 462: 739-744.